

Thermoelastic Equation of State of Boron Suboxide B₆O up to 6 GPa and 2700 K: Simplified Anderson-Grüneisen Model and Thermodynamic Consistency

O.O. Kurakevych,^a and V.L. Solozhenko^{b,*}

^a IMPMC, Sorbonne Universités – UPMC Univ Paris 6, Paris, France

^b LSPM–CNRS, Université Paris Nord, Villetaneuse, France

p-V-T equation of state of superhard boron suboxide B₆O has been measured up to 6 GPa and 2700 K using multianvil technique and synchrotron X-ray diffraction. To fit the experimental data, the theoretical p-V-T equation of state has been derived in approximation of the constant value of the Anderson-Grüneisen parameter δ_T . The model includes bulk modulus $B_0 = 181$ GPa and its first pressure derivative $B_0' = 6$ at 300 K; two parameters describing thermal expansion at 0.1 MPa, i.e. $a = 1.4 \cdot 10^{-5} K^{-1}$ and $b = 5 \cdot 10^{-9} K^{-2}$, as well as $\delta_T = 6$. The good agreement between fitted and experimental isobars has been achieved to the absolute volume changes up to 5% as compared to volume at standard conditions, V_0 . The fitted thermal expansion at 0.1 MPa is well consistent with the experimental data, as well as with ambient-pressure heat capacity c_p , bulk modulus B_0 and δ_T describing its evolution with volume and temperature. The fitted value of Grüneisen parameter $\gamma = 0.85$ is in agreement with previous empiric estimations for B₆O and experimental values for other boron-rich solids.

Keywords: boron suboxide, equation of state, high pressure, high temperature.

Introduction.

Boron-oxygen system is very promising for both fundamental physics and chemistry, as well as for materials science [1]. Very unusual thermodynamic and kinetic properties of boron oxide B₂O₃ has been reported [2-5]; a number of intriguing compounds has been predicted [6-8], while to the present time only boron suboxide B₆O has been synthesized and characterized [9-14]. Although the thermodynamics of boron at both ambient and high pressure has been recently studied quite thoroughly [15], the majority of boron-rich solids remains poorly investigated, especially, the phases that are synthesized at high pressure.

Boron suboxide B₆O [9] is a superhard phase that is usually obtained by high pressure – high temperature synthesis [12,16]. B₆O crystallizes in a $R\bar{3}m$ space group and is able to form unusual multiply-twinned crystals with icosahedral habit [17]. The B₁₂ icosahedra form a distorted cubic close packing (ccp) with O-atoms connecting the icosahedra along the [111] rhombohedra direction [14]. B₆O combines low density, high hardness and chemical inertness that are useful for shaping materials and high-wear application [18-20]; and unique thermal and electronic properties that may be useful for thermoelectric power generation [21]. At present the

* e-mail: vladimir.solozhenko@univ-paris13.fr

300-K equation of state to 60 GPa [22], data on the heat capacity to 800 K [23] and some other thermodynamic properties [12,18] of B₆O are established. Still, the experimental high pressure – high temperature thermodynamic data are lacking, which render difficult predictions and synthesis of new challenging materials, for example, in the B–N–O system at high pressures [24].

In our previous study [18] we analyzed the available heat capacity data and fitted them to the adaptive pseudo-Debye model proposed by Holtzapfel (see [25] for details):

$$c_p = 3R\tau^3 \frac{4C_0 + 3C_1\tau + 2C_2\tau^2 + C_3\tau^3}{(C_0 + C_1\tau + C_2\tau^2 + C_3\tau^3)^2} \left[1 + A \frac{\tau^4}{(a + \tau)^3} \right] \quad \text{Eq. 1}$$

where $\tau = T/\theta_h$; θ_h is Debye temperature in the high-temperature region; C_1 , C_2 and A are parameters to be fitted; $C_3 = 1$; a characterizes non-harmonicity and was fixed to 1/8; R is gas constant. Parameter C_0 has been chosen as $C_0 = (5\theta_l^3)/(\pi^4\theta_h^3)$, with θ_l and θ_h Debye temperatures in the low- and high-temperature regions, respectively, in order to obtain these values directly as fitting parameters. The fitting gave $\theta_h = 1020$ K, $\theta_l = 1175$ K, $C_1 = -0.0865$, $C_2 = 1$, and $A = 0.125$. These values allowed establishing the best standard values of $c_p = 10.24$ J mol⁻¹ K⁻¹, $H^\circ - H_0^\circ = 1.147$ kJ mol⁻¹ and $S^\circ - S_0^\circ = 5.621$ J mol⁻¹ K⁻¹ [18]. Very recently, the new data on B₆O heat capacity has been reported [26], and it would be important to improve our thermodynamic vision of B₆O and check the challenging predictions [18].

The p - V - T equation of state is required to calculate the thermodynamic potentials at high pressures according to the method described elsewhere [11,27]. In the present work we have measured the thermal expansion of B₆O in the 300-2700 K temperature range at pressures up to 6 GPa. Based on these data, the thermoelastic equation of state of B₆O has been proposed.

Experimental.

Boron suboxide has been synthesized by the reaction of β -rhombohedral boron with B₂O₃ at 6 GPa and 2000 K (5-min heating) using a toroid-type high-pressure apparatus according to the procedure described in [13]. The recovered sample has reddish-brown color. X-ray powder diffraction (Seifert MZIII, Bragg-Brentano geometry, CuK α radiation) indicated that the sample contains only highly crystalline B₆O phase. According to the full profile analysis of the diffraction pattern, the lattice parameters are $a = 5.385(2)$ Å, $c = 12.32(1)$ Å) i.e. close to the values reported in [13]. Thus, the oxygen deficiency in as-synthesized B₆O sample is negligible, because the dependence of lattice parameters on concentration of oxygen vacancies is

significant, i.e. $da/dx = 0.083 \text{ \AA}$ and $dc/dx = -0.117 \text{ \AA}$ (see the detailed sample characterization in [10]).

In situ high-pressure experiments up to 6 GPa were carried out using a multianvil X-ray system MAX80 at beamline F2.1, HASYLAB-DESY. The experimental setup has been described elsewhere [28]. Energy-dispersive data were collected on a Canberra solid state Ge-detector with fixed Bragg angle $2\theta = 9.110(3)^\circ$ using a white beam collimated down to $60 \times 100 \mu\text{m}^2$ (vertical by horizontal) and the detector optics with 2θ acceptance angle of 0.005° , which ensures a high resolution of the observed diffraction patterns. The detector was calibrated using the K_α and K_β fluorescence lines of Cu, Rb, Mo, Ag, Ba, and Tb. To decrease the deviatoric stress that was generated during "cold" compression and thus attain quasi-hydrostatic pressure condition during equation-of-state measurements, the samples were pre-annealed at 800 K and a given pressure for 10 min. The sample pressure was determined from the c lattice parameter of highly-ordered hBN using the corresponding equation of state reported in [29] and/or by the equation of state of B_6O [22]. The temperature was measured by W3%Re–W25%Re thermocouple (without correction for the pressure effect on the thermocouple emf) and estimated using power–temperature calibration curve at temperatures above the thermocouple melting. Additionally, CsCl melting curve [30] was used as a control in some experiments.

Results and Discussion.

Experimental data.

The energy-dispersive diffraction patterns of B_6O show three well-defined lines, i.e. 003 , 104 and 021 , that were used for the estimation of lattice parameters and unit cell volumes at each experimental point (Fig. 1a). The temperature dependences of the relative volume V/V_0 (V_0 corresponds to 300 K and ambient pressure) at different pressures are shown in Fig. 2. In the 300–2500 K range the dependences are very close to linear (the points at 300 K correspond to the equation of state measured in [22]). The slopes, however, remarkably depend on pressure.

At temperatures above 2500 K, the strong weakening of 003 and surrounding (101 and 012) reflections has been occasionally observed (Fig. 1a). Similar patterns have been previously reported in the case of the B–N system [31,32], but they do not belong to any phase of the "B₆O-type" or to more general " α -boron related" structures [33,34]. The appearance of a new phase may be the reason why some point at highest temperatures deviate from the theoretical equations of state. However, some pressure drop can be also a reason for that. Here for processing of the equation-of-state data we have used only characteristic diffraction patterns of B_6O .

Simplified Anderson-Grüneisen model.

For the fit of the thermoelastic data, we have used the Anderson-Grüneisen model [35] combined with the results of [36,67] (see [38] for details and physical reasoning), i.e.

$$\alpha(p, T) = \alpha(0, T) \left[\frac{V(p, T)}{V(0, T)} \right]^{\delta_T} \quad \text{Eq. 2}$$

or, in the terms of bulk modulus,

$$B(p, T) = B(p, 300) \left[\frac{V(p, T)}{V(p, 300)} \right]^{-\delta_T} \quad \text{Eq. 3}$$

If δ_T for both thermal expansion and bulk modulus is constant, Eq. 2 can be easily transformed (using the definition of thermal expansion) into

$$\int_{T_1}^{T_2} d[V(p, T)]^{-\delta_T} = \int_{T_1}^{T_2} d[V(0, T)]^{-\delta_T}, \quad \text{Eq. 4}$$

and, therefore, we obtain

$$V(p, T) = \left[V(0, T)^{-\delta_T} + V(p, 300)^{-\delta_T} - V(0, 300)^{-\delta_T} \right]^{-1/\delta_T}. \quad \text{Eq. 5}$$

To a good approximation the above relationships can be used when the volume change due to compression/thermal dilatation does not exceed 5-10%, i.e. when Eqs. 2 & 3 are valid [39].

During fitting procedure, the $V(0, T)$ dependence [40,41] has been suggested to follow equation

$$V(0, T) = V(0, 300) [1 + a (T-300) + b (T-300)^2], \quad \text{Eq. 6}$$

while the $V(p, 300)$ dependence has been fixed to the 300-K equation of state of B₆O reported in [22].

Fitting all available experimental p - V - T data to Eq. 5 leads to $\delta_T = 6$, $a = 1.4 \cdot 10^{-5} \text{ K}^{-1}$, $b = 5 \cdot 10^{-9} \text{ K}^{-2}$, while $V(p, 300)$ is defined by Vinet equation of state [42]:

$$p = 3B_0 (V/V_0)^{-2/3} \left[1 - (V/V_0)^{1/3} \right] e^{1.5 (B'_0 - 1) \left[1 - (V/V_0)^{1/3} \right]} \quad \text{Eq. 7}$$

with $B_0 = 181 \text{ GPa}$ and $B'_0 = 6$ [22].

Thermal expansion coefficient and bulk modulus at high pressure and high temperature.

The pressure dependence of mean thermal expansion and temperature dependence of bulk modulus are shown in Figs. 3a and 3b, respectively. The experimental data (symbols) well fit the curves calculated using the model represented by equations (1) and (2). The thermal expansion at 0.1 MPa and 2000 K (the mean value of the 1500-2500 K region) should be 3.4 K^{-1} using a - and b -coefficients described above. This value is in a good agreement with 3.6 K^{-1} , obtained by exponential extrapolation of our experimental data down to 0.1 MPa (Fig. 3a), which additionally validates our thermoelastic equation of state. The mean high-temperature α as a function of pressure well follows the exponential dependence:

$$\langle \alpha \rangle = 3.567 \cdot 10^{-5} \cdot e^{-0.09546 p}. \quad \text{Eq. 8}$$

Thus, B_0O volume at given p - T conditions may also be calculated using the following approximate equation:

$$V(T, p) = V(300, p) \cdot \exp\left(3.567 \cdot 10^{-5} \cdot e^{-0.09546 p} \cdot (T - 300)\right). \quad \text{Eq. 9}$$

This equation allows us to make a good estimation for high-temperature behavior of bulk modulus, i.e.

$$\left(\frac{\partial \alpha}{\partial p}\right)_T = \left(\frac{\partial}{\partial p} \left(\frac{\partial \ln V}{\partial T}\right)_p\right)_T = \left(\frac{\partial}{\partial T} \left(\frac{\partial \ln V}{\partial p}\right)_T\right)_p = \left(\frac{\partial}{\partial T} \left(\frac{1}{B}\right)_T\right)_p \quad \text{Eq. 10}$$

and, after integration over the temperature,

$$\int_{300}^T \left(\frac{\partial \alpha}{\partial p}\right)_T dT = \frac{1}{B_0(T)} - \frac{1}{B_0(300K)} \quad \text{Eq. 11}$$

and the temperature dependence of a bulk modulus is expressed by equation

$$B_0(T) = \frac{B_0(300K)}{1 - B_0(300K) \int_{300}^T \left(\frac{\partial \alpha}{\partial p}\right)_T dT}. \quad \text{Eq. 12}$$

The pressure derivative of the thermal expansion coefficient does not depend on temperature (at least, for mean values at high temperatures); so the zero-pressure bulk modulus of B_0O should change with temperature according to equation

$$B_0(T) \cong \frac{B_0(300K)}{1 + B_0(300K) \cdot 3.403 \cdot 10^{-6} (T - 300)}. \quad \text{Eq. 13}$$

The temperature dependence of B_0 is illustrated in Fig. 3. Two values of $B_0(300)$, 181 GPa [22] and 217 GPa (the value suggested by McMillan, private communication), have been used for the construction of the theoretical curves (Eq. 13). The bulk moduli were established at high (1000-2000 K) temperatures by fitting the p - V data to the Murnaghan equation [43] at a given temperature (B_0' fixed to 6 and independent of temperature). When the Vinet equation was used, the difference with the Murnaghan equation is less than 0.5%, at least up to 10 GPa. Thus, our high pressure – high temperature data well agree with room-temperature equation of state reported in [22], and can serve an independent confirmation of the 300-K bulk modulus value of $B_0 = 181$ GPa.

Thermodynamic consistency of equation of state.

The thermodynamic consistency of thus established p - V - T equation of state and heat capacity c_p experimental data [18,23,26] has been verified. The relationship between thermal expansion and heat capacity c_v may be expressed as

$$\alpha = \frac{\gamma \cdot c_v}{B \cdot V}, \quad \text{Eq. 14}$$

where γ is Grüneisen parameter and B is isothermal bulk modulus. Heat capacity c_p is given by the following equations:

$$c_p = c_v + \alpha^2 BTV \quad \text{and} \quad c_p = \alpha \frac{BV}{\gamma} + \alpha^2 BTV, \quad \text{Eq. 15}$$

and, hence, thermal expansion can be expressed as

$$\alpha = \frac{1}{2\gamma T} \left(\sqrt{1 + \frac{4c_p \gamma^2 T}{BV}} - 1 \right) \quad \text{Eq. 16}$$

Now, we can integrate Eq. 16 and obtain the integral functional equation in respect to $V(T)$:

$$\ln \frac{V(T)}{V_0} = \int_{T_0}^T \frac{1}{2\gamma\tau} \left(\sqrt{1 + \frac{4c_p(\tau) \gamma^2 \tau V_0^{\delta_\tau}}{B_0 [V(\tau)]^{\delta_\tau+1}}} - 1 \right) d\tau \quad \text{Eq. 17}$$

In order to solve Eq. 17 in respect to $V(T)$, one can easily use the iteration method

$$V_{i+1}(T) = f(V_i(T), \gamma). \quad \text{Eq. 18}$$

where

$$f(V(T), \gamma) = V_0 \exp \left\{ \int_{T_0}^T \frac{1}{2\gamma\tau} \left(\sqrt{1 + \frac{4c_p(\tau) \gamma^2 \tau V_0^{\delta_T}}{B_0 [V(\tau)]^{\delta_T+1}}} - 1 \right) d\tau \right\} \quad \text{Eq. 19}$$

Parameter γ in Eqs. 17-19 remains unknown and should be fitted, contrary to δ_T , V_0 at 300 K and 0.1 MPa, and $c_p(T)$. As first approximation of the $V_I(T)$ function we took the dependence defined by Eq. 6. Five iterations usually give a stable solution of Eq. 17, i.e. $V(T) \cong V_5(T) \pm 0.1\%$.

Fig. 4a shows the heat capacity c_p of B_6O as a function of temperature. Three experimental sets of data are presented: one corresponding to the low-temperature measurements [23], one high-temperature set up to 780 K [23] and very recent data up to 1250 K [26]. The latter gives higher heat capacity values in the high-temperature range, and the fitting parameters for Eq. 1 are $\theta_h = 1075$ K, $\theta_l = 1275$ K, $C_1 = -0.05$, $C_2 = 0.75$, and $A = 0.10$. These new heat capacity data show the best agreement with experimental $V(T)$ dependence [40,41] (Fig. 4b). The Grüneisen parameter γ can be estimated as 0.85 (high-temperature limit), in a reasonable agreement with previous empirical estimations of $\sim 0.75(15)$ (mean value over the 50-1500 K range) [40,41].

Conclusions.

Thermal expansion of B_6O has been studied in the 300-2700 K temperature range at pressures from 2 to 6 GPa. Based on these data, thermoelastic equation of state has been constructed which is well consistent with independent experimental data on 300-K equation of state and thermal expansion at 0.1 MPa. To fit the experimental data, the theoretical p - V - T equation of state of B_6O has been proposed. The model implies the constant value of Anderson-Grüneisen parameter $\delta_T = 6$; bulk modulus $B_0 = 181$ GPa and its first pressure derivative $B_0' = 6$ at 300 K; and two parameters describing the thermal expansion at 0.1 MPa, i.e. $a = 1.4 \cdot 10^{-5} \text{ K}^{-1}$ and $b = 5 \cdot 10^{-9} \text{ K}^{-2}$.

Acknowledgements. *In situ* experiments at HASYLAB-DESY have been performed during beamtime allocated to Projects DESY-D-I-20080149 EC and DESY-D-I-20120445 EC and received funding from the European Community's Seventh Framework Programme (FP7/2007-2013) under grant agreement n° 226716. This work was financially supported by the Agence Nationale de la Recherche (grant ANR-2011-BS08-018).

References

1. *Kurakevych, O.O.* Superhard phases of simple substances and binary compounds of the B-C-N-O system: from diamond to the latest results (a Review) // *J. Superhard Mater.* - 2009. - **31**, No 3. - P. 139-157.
2. *Brazhkin, V.V., Farnan, I., Funakoshi, K., Kanzaki, M., Katayama, Y., Lyapin, A.G., Saitoh, H.* Structural transformations and anomalous viscosity in the B₂O₃ melt under high pressure. // *Phys. Rev. Lett.* - 2010. - **105**, No 11. - P. 115701.
3. *Brazhkin, V.V., Tsiok, O.B., Katayama, Y.* Investigation of polyamorphism in compressed B₂O₃ glass by the direct measurement of the density. // *JETP Lett.* - 2009. - **89**, No 5. - P. 244-248.
4. *Brazhkin, V.V., Katayama, Y., Inamura, Y., Kondrin, M.V., Lyapin, A.G., Popova, S.V., Voloshin, R.N.* Structural transformations in liquid, crystalline, and glassy B₂O₃ under high pressure. // *JETP Lett.* - 2003. - **78**, No 6. - P. 393-397.
5. *Aziz, M.J., Nygren, E., Hays, J.F., Turnbull, D.* Crystal-growth kinetics of boron-oxide under pressure. // *J. Appl. Phys.* - 1985. - **57**, No 6. - P. 2233-2242.
6. *Mukhanov, V.A., Kurakevich, O.O., Solozhenko, V.L.* On the hardness of boron (III) oxide. // *J. Superhard Mater.* - 2008. - **32**, No 1. - P. 71-72.
7. *Endo, T., Sato, T., Shimada, M.* High-pressure synthesis of B₂O with diamond-like structure. // *J. Mater. Res. Lett.* - 1987. - **6** - P. 683-685.
8. *Nelmes, R.J., Loveday, J.S., Wilson, R.M., Marshall, W.G., Besson, J.M., Klotz, S., Hamel, G., Aselage, T.L., Hull, S.* Observation of inverted-molecular compression in boron carbide. // *Phys. Rev. Lett.* - 1995. - **74**, No 12. - P. 2268.
9. *Rizzo, H.F., Simmons, W.C., Bielstein, H.O.* The existence and formation of the solid B₆O. // *J. Electrochem. Soc.* - 1962. - **109**, No 11. - P. 1079-1082
10. *Solozhenko, V.L., Kurakevych, O.O., Bouvier, P.* First and second order Raman scattering of B₆O. // *J. Raman Spectr.* - 2009. - **40**, No 8. - P. 1078-1081.
11. *Solozhenko, V.L., Kurakevych, O.O., Turkevich, V.Z., Turkevich, D.V.* Phase diagram of the B-B₂O₃ system at 5 GPa: Experimental and theoretical studies. // *J. Phys. Chem. B* - 2008. - **112**, No 21. - P. 6683-6687.
12. *McMillan, P.F., Hubert, H., Chizmeshya, A., Petuskey, W.T., Garvie, L.A.J., Devouard, B.* Nucleation and growth of icosahedral boron suboxide clusters at high pressure. // *J. Solid State Chem.* - 1999. - **147**, No 1. - P. 281-290.
13. *Hubert, H., Garvie, L.A.J., Devouard, B., Buseck, P.R., Petuskey, W.T., McMillan, P.F.* High-pressure, high-temperature synthesis and characterization of boron suboxide (B₆O). // *Chem. Mater.* - 1998. - **10**, No 6. - P. 1530-1537.
14. *Kobayashi, M., Higashi, I., Brodhag, C., Thevenot, F.* Structure of B₆O boron suboxide by Rietveld refinement. // *J. Mater. Sci.* - 1993. - **28**, No 8. - P. 2129-2134.
15. *Solozhenko, V.L., Kurakevych, O.O.* Equilibrium p-T phase diagram of boron: Experimental study and thermodynamic analysis. // *Sci. Rep.* - 2013. - **3** - art. 2351.

16. *McMillan, P.F.* New materials from high-pressure experiments. // *Nat. Mater.* - 2002. - **1**, No 1. - P. 19-25.
17. *Hubert, H., Devouard, B., Garvie, L.A.J., O'Keeffe, M., Buseck, P.R., Petuskey, W.T., McMillan, P.F.* Icosahedral packing of B-12 icosahedra in boron suboxide (B_6O). // *Nature* - 1998. - **391**, No 6665. - P. 376-378.
18. *Kurakevych, O.O., Solozhenko, V.L.* Experimental study and critical review of structural, thermodynamic and mechanical properties of superhard refractory boron suboxide B_6O . // *J. Superhard Mater.* - 2011. - **33**, No 6. - P. 421-428.
19. *Veprek, S., Zhanga, R.F.* Mechanical properties and hardness of boron and boron-rich solids. // *J. Superhard Mater.* - 2011. - **33**, No 6. - P. 409-420.
20. *Mukhanov, V.A., Kurakevych, O.O., Solozhenko, V.L.* Thermodynamic model of hardness: Particular case of boron-rich solids. // *J. Superhard Mater.* - 2010. - **32**, No 3. - P. 167-176.
21. *Emin, D.* Icosahedral boron-rich solids as refractory semiconductors // in *Novel Refractory Semiconductors* (D. Emin, T.L. Aselage, C. Woods, eds.), Materials Research Society Symposia Proceedings. - 1987. - **97**. - P. 3-16.
22. *Nieto-Sanz, D., Loubeyre, P., Crichton, W., Mezouar, M.* X-ray study of the synthesis of boron oxides at high pressure: phase diagram and equation of state. // *Phys. Rev. B* - 2004. - **70**, No 21 - P. 214108 1-6.
23. *Tsagareishvili, G.V., Tsagareishvili, D.S., Tushishvili, M.C., Opmiadze, I.S., Naumov, V.N., Tagaev, A.B.* Thermodynamic properties of boron suboxide in the temperature range 11.44-781.8 K. // *AIP Conf. Proc.* - 1991. - **231** - P. 384-391.
24. *Solozhenko, V.L., Turkevich, V.Z., Kurakevych, O.O., Turkevich, D.V., Taniguchi, T.* Phase equilibria in the B-BN- B_2O_3 system at 5 GPa. // *J. Phys. Chem. C* - 2013. - **117**, No 36. - P. 18642-18647.
25. *Solozhenko, V.L., Turkevich, V.Z., Holzappel, W.B.* Refined phase diagram of boron nitride. // *J. Phys. Chem. B* - 1999. - **103**, No 15. - P. 2903-2905.
26. *Thiele, M., Herrmann, M., Raethel, J., Kleebe, H.-J., Mueller, M.M., Gestrich, T., Michaelis, A.* Preparation and properties of B_6O/TiB_2 -composites. // *J. Europ. Ceram. Soc.* - 2012. - **32**, No 8. - P. 1821-1835.
27. *Solozhenko, V.L., Kurakevych, O.O., Turkevich, V.Z., Turkevich, D.V.* Phase diagram of the B-BN system at 5 GPa. // *J. Phys. Chem. B* - 2010. - **114**, No 17. - P. 5819-5822.
28. *Shimomura, O.* Current activity of MAX80 at the Photon Factory. // *Physica B+C* - 1986. - **139-140**, No 1. - P. 292-300.
29. *Solozhenko, V.L., Will, G., Elf, F.* Isothermal compression of hexagonal graphite-like boron nitride up to 12 GPa. // *Solid State Comm.* - 1995. - **96**, No 1. - P. 1-3.
30. *Vaidya, S.N., Kennedy, G.C.* Effect of pressure on the melting of cesium chloride. // *J. Phys. Chem. Solids* - 1971. - **32**, No 10. - P. 2301-2304.
31. *Hubert, H., Garvie, L.A.J., Buseck, P.R., Petuskey, W.T., McMillan, P.F.* High-pressure, high-temperature syntheses in the B-C-N-O system - I. Preparation and characterization. // *J. Solid State Chem.* - 1997. - **133**, No 2. - P. 356-364.

32. *Solozhenko, V.L., Kurakevych, O.O.* Chemical interaction in the B-BN system at high pressures and temperatures. Synthesis of novel boron subnitrides. // *J. Solid State Chem.* - 2009. - **182**, No 6. - P. 1359-1364.
33. *Solozhenko, V.L., Le Godec, Y., Kurakevych, O.O.* Solid-state synthesis of boron subnitride, B₆N: myth or reality? // *C. R. Chimie* - 2006. - **9**, No 11-12. - P. 1472-1475.
34. *Kurakevych, O.O., Solozhenko, V.L.* Rhombohedral boron subnitride, B₁₃N₂, by X-ray powder diffraction. // *Acta Crystallogr. C* - 2007. - **63**, No 9. - P. i80-i82.
35. *Anderson, O.L., Isaak, D.G.* The dependence of the Anderson-Grueneisen parameter δ_T upon compression at extreme conditions. // *J. Phys. Chem. Solids* - 1993. - **54**, No 2. - P. 221-227.
36. *Burakovsky, L., Preston, D.L.* Analytic model of the Grueneisen parameter all densities. // *J. Phys. Chem. Solids* - 2004. - **65**, No 8-9. - P. 1581-1587.
37. *Tallon, J.L.* The thermodynamics of elastic deformation - I: Equation of state for solids. // *J. Phys. Chem. Solids* - 1980. - **41**, No 8. - P. 837-850.
38. *Shanker, J., Singh, B.P., Jitendra, K.* Analysis of thermal expansivity of solids at extreme compression. // *Condensed Matter Physics* - 2008. - **11**, No 4. - P. 681-686.
39. *Anderson, O., Oda, H., Chopelas, A., Isaak, D.* A thermodynamic theory of the Grueneisen ratio at extreme conditions: MgO as an example. // *Phys. Chem. Minerals* - 1993. - **19**, No 6. - P. 369-380.
40. *Tsagareishvili, D.S., Tushishvili, M.C., Tsagareishvili, G.V.* Estimation of some thermoelastic properties of boron suboxide in wide ranges of temperature. // *AIP Conf. Proc.* - 1991. - **231**, No 1. - P. 392-395.
41. *Tushishvili, M.C., Tsagareishvili, G.V., Tsagareishvili, D.S.* Thermoelastic properties of boron suboxide in the 0-1500 K range. // *J. Hard Mater.* - 1992. - **3** - P. 225-233.
42. *Vinet, P., Ferrante, J., Smith, J.R., Rose, J.H.* A Universal equation of state for solids. // *J. Phys. C* - 1986. - **19**, No 20. - P. L467-L473.
43. *Murnaghan, F.D.* The compressibility of media under extreme pressures. // *Proct. Natl. Acad. Sci.* - 1944. - **30**, No 9. - P. 244.

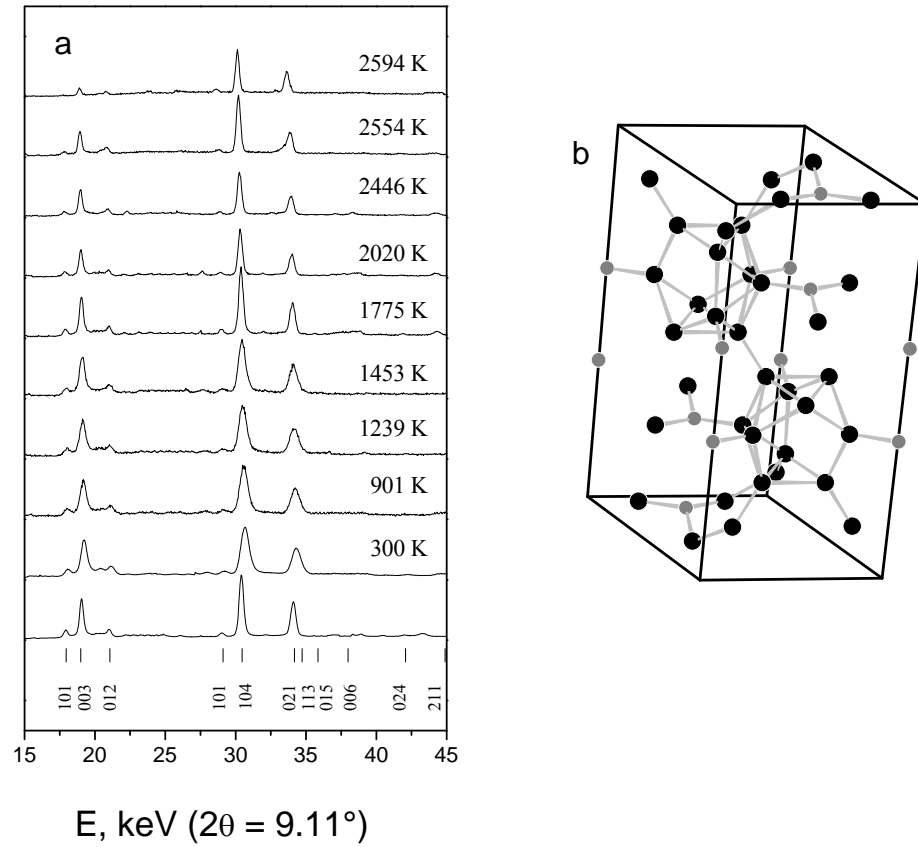


Figure 1. (a) Energy-dispersive diffraction patterns of B_6O taken *in situ* at 4.3 GPa upon heating to 2600 K (the bottom pattern is taken at ambient conditions). (b) Crystal structure of B_6O . Black and grey balls represent boron and oxygen atoms, respectively.

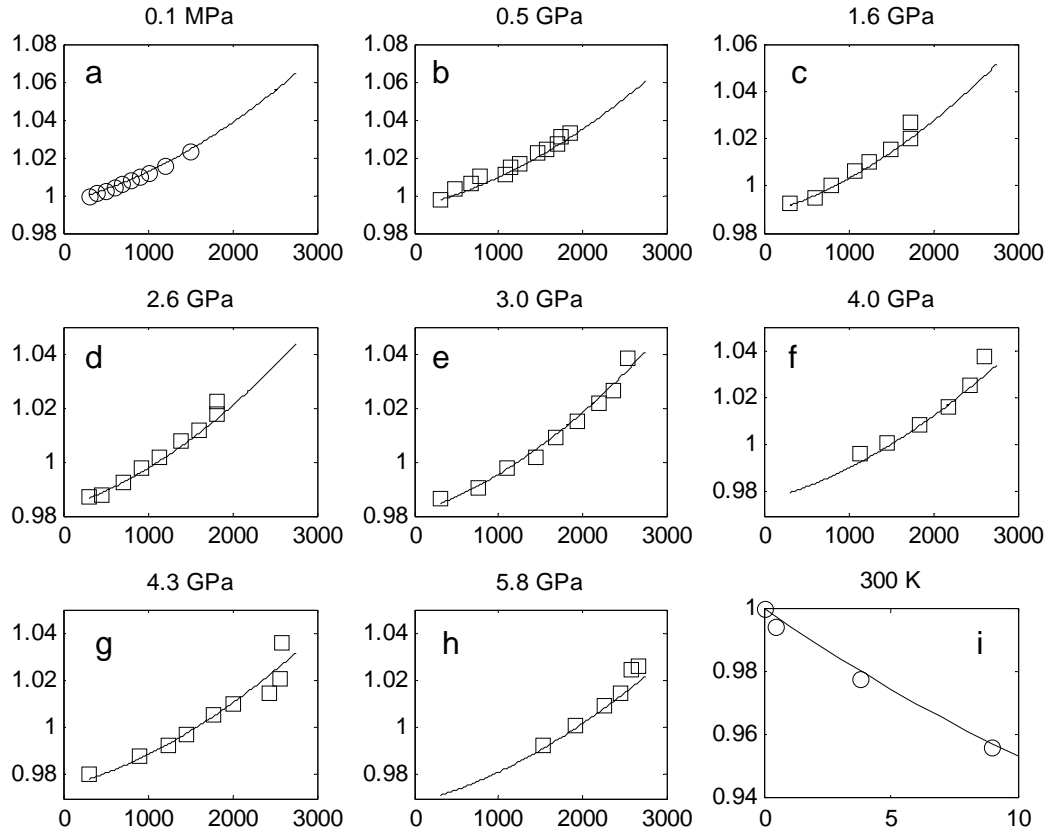


Figure 2. (a - h) Temperature dependence of relative volume V/V_0 of B_6O (V_0 taken at 300 K and ambient pressure). The plot coordinates are $x - T$ (K) and $y - V/V_0$. (i) Pressure dependence of relative volume V/V_0 of B_6O at 300 K. The plot coordinates are $x - p$ (GPa) and $y - V/V_0$.

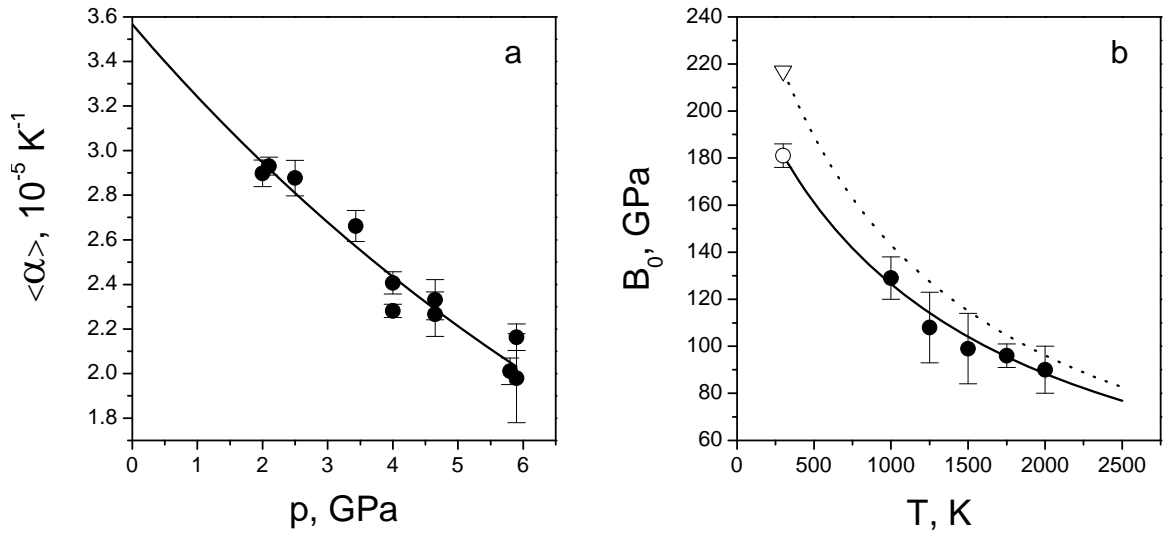


Figure 3. Experimental data on (a) pressure dependence of the mean high-temperature coefficient of thermal expansion of B_6O (solid line shows the exponential fit) and (b) temperature dependence of the bulk modulus of B_6O (solid line corresponds to the theoretical line with $B_0 = 181 \text{ GPa}$, while dotted line, to $B_0 = 217 \text{ GPa}$ at 300 K). Solid symbols represent our results, open symbols are literature data [22].

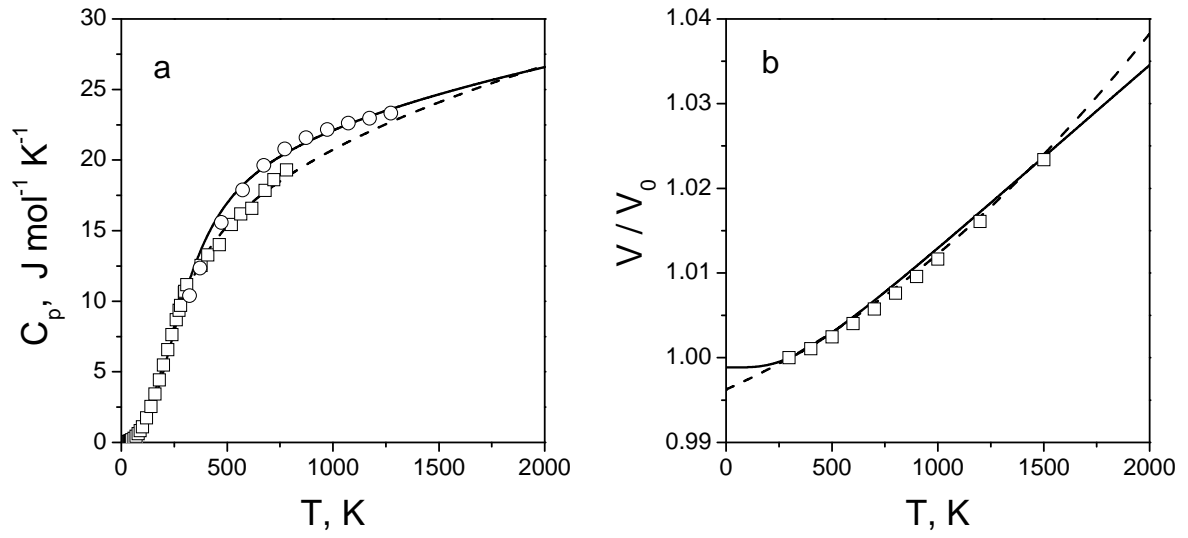


Figure 4. Experimental data on (a) heat capacity c_p of B₆O as a function of temperature (squares from [23], circles from [26], lines show the results of fitting to Eq. 1); and (b) thermal expansion of B₆O at 0.1 MPa (squares are experimental data [41], dashed curve corresponds to the square-polynomial fitting (Eq. 6), while solid one – to the numerical solution of Eq. 17 with Grüneisen coefficient $\gamma = 0.85$).